JOURNAL OF VIROLOGY, Oct. 2007, p. 10792–10803 Vol. 81, No. 19
0022-538X/07/$08.00+0 doi:10.1128/JVI.00196-07

Emerin Is Hyperphosphorylated and Redistributed in Herpes Simplex Virus Type 1-Infected Cells in a Manner Dependent on both UL34 and US3[▽]

Natalie Leach,[1] Susan L. Bjerke,[2] Desire K. Christensen,[2] Jacques M. Bouchard,[2] Fan Mou,[3] Richard Park,[3] Joel Baines,[3] Tokuko Haraguchi,[4] and Richard J. Roller[2]*

Program in Molecular and Cellular Biology, University of Iowa, Iowa City, Iowa 52242[1]; Department of Microbiology, University of Iowa, Iowa City, Iowa 52242[2]; Department of Microbiology and Immunology, Cornell University, Ithaca, New York 14853[3]; and CREST Research Project, Kansai Advanced Research Center, National Institute of Information and Communications Technology, 588-2 Iwaoka, Iwaoka-cho, Nishi-ku, Kobe 651-2492, Japan[4]

Received 29 January 2007/Accepted 5 July 2007

Cells infected with wild-type herpes simplex virus type 1 (HSV-1) show disruption of the organization of the nuclear lamina that underlies the nuclear envelope. This disruption is reflected in changes in the localization and phosphorylation of lamin proteins. Here, we show that HSV-1 infection causes relocalization of the LEM domain protein emerin. In cells infected with wild-type virus, emerin becomes more mobile in the nuclear membrane, and in cells infected with viruses that fail to express UL34 protein (pUL34) and US3 protein (pUS3), emerin no longer colocalizes with lamins, suggesting that infection causes a loss of connection between emerin and the lamina. Infection causes hyperphosphorylation of emerin in a manner dependent upon both pUL34 and pUS3. Some emerin hyperphosphorylation can be inhibited by the protein kinase Cδ (PKCδ) inhibitor rottlerin. Emerin and pUL34 interact physically, as shown by pull-down and coimmunoprecipitation assays. Emerin expression is not, however, necessary for infection, since virus growth is not impaired in cells derived from emerin-null transgenic mice. The results suggest a model in which pUS3 and PKCδ that has been recruited by pUL34 hyperphosphorylate emerin, leading to disruption of its connections with lamin proteins and contributing to the disruption of the nuclear lamina. Changes in emerin localization, nuclear shape, and lamin organization characteristic of cells infected with wild-type HSV-1 also occur in cells infected with recombinant virus that does not make viral capsids, suggesting that these changes occur independently of capsid envelopment.

During primary envelopment, herpes simplex virus type 1 (HSV-1) nucleocapsids translocate from the nucleus to the cytoplasm by budding into the inner nuclear membrane and then fusing with the outer nuclear membrane. The capsid does not, however, have unimpeded access to the inner nuclear membrane. Lining the inside of the inner nuclear membrane is the nuclear lamina, which is composed of a meshwork of proteins with spaces too small for the capsid to move through without some disruption (2, 19, 65). The lamina meshwork is made up of intermediate filament family proteins called lamins that are linked to the inner nuclear membrane and to intranuclear proteins by association with lamin-associated proteins (LAPs) (reviewed in reference 65). Connection of the network of lamin proteins to the inner nuclear membrane is mediated by integral membrane LAPs, including emerin, lamin B receptor, LAP2-β, and MAN-1 (26).

Emerin is a member of a family of nuclear envelope proteins that share a common sequence called the LEM domain that mediates association with BAF (barrier to autointegration factor) and is important for the assembly of LEM domain proteins into the re-forming nuclear envelope following mitosis (21, 37, 39). Emerin also contains a lamin-binding domain that helps retain it in the interphase nuclear envelope (6, 14, 25, 37). Emerin is ubiquitously expressed but is not essential for the viability of cells in culture (36). Failure to express or properly localize emerin in humans, however, is one cause of Emery-Dreifuss muscular dystrophy (EDMD) (3, 14). The relationship between abnormalities in emerin and the pathogenesis of EDMD is not clear. Mice with deletions in the gene encoding emerin develop apparently normally but show defects in muscle regeneration and subtle defects in motor coordination (40, 47).

HSV-1 UL34 protein (pUL34) forms part of an envelopment complex that also includes pUL31 and pUS3. All three proteins colocalize at the nuclear membrane, and each is necessary for normal localization of the others in infected cells (51, 54). pUL34 and pUL31 can colocalize at the nuclear membrane in the absence of other viral proteins (52, 66). pUL34 also interacts with and forms a complex with pUL31 in vitro, and the interaction between the proteins is a conserved feature of herpesviruses (35, 52, 59). pUL34, pUL31, and their homologs in other herpesviruses are necessary for efficient envelopment at the inner nuclear membrane (15, 18, 33, 46, 52, 54). pUS3 is not necessary for envelopment but plays a role in de-envelopment of capsids in the perinuclear space into the cytoplasm (53, 63).

One function of the envelopment complex is to mediate reorganization of the nuclear lamina. pUL34, pUL31, and

* Corresponding author. Mailing address: Department of Microbiology, The University of Iowa, 3-432 Bowen Science Building, Iowa City, IA 52242. Phone: (319) 335-9958. Fax: (319) 335-9006. E-mail: richard-roller@uiowa.edu.

▽ Published ahead of print on 25 July 2007.

their murine cytomegalovirus (MCMV) homologs have been shown to be required for changes in nuclear shape and size and for changes in the distribution of nuclear lamin A/C and lamin B proteins in infected and transfected cells (4, 45, 48, 51, 62). HSV-1 pUS3 negatively regulates disruption of the nuclear lamina. In its absence, large perforations form in the network of lamin proteins (4). Overexpression of pUL34 in transient transfection results in disruption of lamin A/C and lamin B organization (51, 61), and the morphology of the nuclear membrane is altered so that the inner and outer membranes are separated (67). These effects are similar to those seen in HSV-1-infected cells. In addition, the location of pUL34 in infected cells at the nuclear membrane places it in an excellent position to interact with and modulate the actions of lamin proteins and LAPs.

It seems likely that in order to achieve its effects on nuclear architecture, HSV must accomplish two things. It must disrupt interactions between the lamin A/C and lamin B proteins that form the lamina meshwork, and it must disrupt interactions between the lamin meshwork and the LAPs that connect it to the inner nuclear membrane. HSV infection has been shown to alter the localization of the integral membrane LAP lamin B receptor and to increase its mobility in the nuclear membrane, suggesting that its connection to the lamin network is disrupted (60).

Disassembly of the nuclear lamina at mitosis is associated with phosphorylation of lamins and of LAPs, including emerin (7, 9, 12, 13, 16, 22, 49). HSV has been shown to induce phosphorylation of the lamin proteins during infection, and this may play a role in the infection-dependent disruptions of the lamin proteins (48). HSV-1 UL34 and MCMV U50 proteins recruit protein kinase C (PKC) isoforms to the nuclear membrane, and these recruited enzymes are responsible for at least some of the phosphorylation of lamins seen in infection (45, 48). It is not known what enzymes are responsible for phosphorylation of LAPs during mitosis.

The observation that herpesviruses recruit cellular kinases that participate in mitotic breakdown of the nuclear lamina suggests a model in which HSV-mediated disruption of the lamina relies largely or exclusively on recruited cellular mechanisms. One prediction of this is that LAPs may also be hyperphosphorylated during infection and that this hyperphosphorylation may be required for dissociation of lamina components. In this study, we tested the hypothesis that emerin is hyperphosphorylated in the HSV-infected cell, that association of emerin with the nuclear lamina is disrupted in infection, and that hyperphosphorylation depends upon components of the nuclear envelopment apparatus.

MATERIALS AND METHODS

Cells and viruses. HEp-2 and Vero cells were maintained as previously described (54). Mouse embryonic fibroblasts (MEF) from male mice with a deletion in the emerin gene on the X chromosome ($Em^{-/y}$) and fibroblasts from a wild-type parental strain male ($Em^{+/y}$) were kindly provided by Colin Stewart (36) and maintained in Dulbecco's modified Eagles' medium supplemented with 10% fetal calf serum. The properties of HSV-1(F), vRR1072 (thymidine kinase-positive UL34-null virus), vRR1202 (US3-null virus), vRR1204 (US3 kinase-dead mutant virus), and repair viruses for vRR1072 and vRR1202 were previously described and characterized (52, 54, 55). The VP5-null virus and complementing cells were the kind gift of Prashant Desai (10).

Plasmids and cell lines. The enhanced green fluorescent protein (EGFP)-emerin fusion plasmid was the kind gift of Yasushi Hiraoka. In order to construct stable clonal cell lines expressing EGFP-emerin, Vero cells were transfected with the EGFP-emerin plasmid and subjected to selection with 100 mg/ml G418 for 2 weeks. Colonies showing nuclear green fluorescence were scraped from the plate, transferred to individual cultures, and amplified.

FRAP. Cells from clonal, stable cell lines expressing EGFP-emerin were imaged on a Zeiss 510 confocal microscope, and fluorescence recovery after photobleaching (FRAP) analysis was conducted using the same settings for each cell. The pinhole was set at 2.48 Airy units, and the 488-nm argon laser was set at 1.5% intensity for imaging. A defined region (referred to as the bleaching area) on the top of each nucleus was bleached with a single scan at 100% laser intensity. Imaging scans were then performed at 10-second intervals. A separate region outside of the area used for bleaching (referred to as the control area) was defined and monitored for photobleaching caused by the imaging scans. The percentage recovery in the bleaching area was corrected for overall bleaching caused by the imaging scans, and a ratio representing the residual fluorescence following bleaching was subtracted so that the percentage recovery for the time point at which bleaching occurred was zero. The following equation was used for each cell at each time point: percentage recovery = $\{[(X_o/X_i)/(C_o/C_i)] - [(X_o/X_b)/(C_b/C_i)]\} \times 100$, where X_o is the intensity of the bleaching area before being bleached, X_i is the intensity of the bleaching area at time point i, C_o is the intensity of the control area before being bleached, C_i is the intensity of the control area at time point i, X_b is the intensity of the bleaching region immediately following the bleaching scan, and C_b is the intensity of the control region immediately following bleaching. Ten cells were analyzed for each condition, and the mean recovery of fluorescence at each time point was plotted.

IF. Indirect immunofluorescence (IF) was performed as previously described, with some variations (4, 52). Cells stained for lamin A/C were fixed with 4% formaldehyde for 20 min and then washed with phosphate-buffered saline (PBS). The cells were permeabilized and blocked in the same step by incubating them in 10% Blokhen (Aves Labs) in IF buffer. Primary antibodies were diluted as follows in IF buffer: chicken anti-UL34, 1:1,000; mouse monoclonal immunoglobulin G (IgG) anti-lamin A/C, 1:1,000 (Santa Cruz Biotechnology); mouse monoclonal anti-emerin, 1:500 (LabVision Corporation). Secondary antibodies were also diluted in IF buffer as follows: Alexa Fluor 594 goat anti-chicken IgG (1:1,000) was used to detect PUL34, Alexa Fluor 488 goat anti-mouse IgG (1:400) was used to detect lamin A/C and emerin, and Alexa Fluor 660 goat anti-rabbit IgG conjugate (1:400) was used to detect emerin. Slo-fade II (Molecular Probes) was used to mount coverslips on glass slides. All confocal microscopy work was done with a Zeiss 510 confocal microscope. All images shown are representative of experiments performed a minimum of three times.

Preparation of nuclear fractions and calf intestinal alkaline phosphatase (CIAP) treatment. Nuclear-lamina fractions were prepared by a modification of the procedure described by Krohne (34). Confluent 150-cm^2 cultures of Vero or HEp-2 cells were infected with 5 PFU/cell of virus for 16 h. The infected cells were washed once with PBS, scraped into 8 ml PBS, and pelleted by centrifugation at 600 rpm for 10 min in a clinical centrifuge. The cells were resuspended in 5 ml 10 mM Tris, pH 7.5, containing protease inhibitors and allowed to swell for 5 minutes at 0°C. The cells were lysed with 10 strokes of a Dounce homogenizer. Nuclei were pelleted at $3,000 \times g$ for 10 min, resuspended in 2 ml digestion buffer I (10 mM Tris, pH 8.5, 2 mM $MgCl_2$, 50 U/ml DNase I, 50 mg/ml RNase, and protease inhibitors), and allowed to react at room temperature for 20 min. The digested nuclei were pelleted at $3,000 \times g$ for 10 min and then washed by resuspension in 2 ml 10 mM Tris, pH 7.5, and recentrifugation. The washed nuclei were resuspended in 2 ml digestion buffer II (10 mM Tris, pH 7.5, 2 mM $MgCl_2$, 50 U/ml DNase I, 50 mg/ml RNase, and protease inhibitors) and allowed to react at room temperature for 20 min. Soluble proteins were extracted from the digested nuclei by resuspending the nuclei in high-salt extraction buffer (10 mM Tris, pH 7.5, 500 mM NaCl, 1 mM dithiothreitol) and incubating them on ice for 10 min. The extracted nuclei were pelleted at $10,000 \times g$ for 10 min and then washed by resuspension and recentrifugation in 10 mM Tris, pH 7.5.

Nuclear-lamina fractions were either solubilized directly in SDS-PAGE sample buffer or first extracted with detergent extraction buffer (10 mM Tris, pH 7.5, 1% Triton X-100, 1 mM dithiothreitol, protease inhibitors) containing various amounts of NaCl.

For CIAP treatment, nuclear-lamina fractions from T25 cultures were extracted with 300 mM NaCl, split into two equal fractions, and then incubated for 1 h at 37°C in the presence or absence of 40 U CIAP (Roche). After digestion, sodium dodecyl sulfate-polyacrylamide gel electrophoresis (SDS-PAGE) sample buffer was added, and samples were fractionated on SDS-PAGE gels.

GST pull-down assays. Approximately 5×10^8 HEp-2 cells were harvested, resuspended in 60 ml ice-cold lysis buffer (50 mM Tris-Cl, pH 8.0, 200 mM NaCl,

1% NP-40, 4 μg/ml aprotinin, 4 μg/ml leupeptin, 4 μg/ml pepstatin, 1 mM phenylmethylsulfonyl fluoride), and passaged several times through an 18-gauge needle. The lysate was centrifuged at 10,000 × *g* for 30 min at 4°C, and the supernatant was aliquoted in 5-ml volumes and stored at −20°C. Glutathione *S*-transferase (GST)-pUL34 fusion protein was prepared as described previously (51). Fifteen ml of HEp-2 cell lysate was incubated for 3 h at 4°C with 800 μg of GST-pUL34 fusion protein or 800 μg GST bound to glutathione-Sepharose beads (Amersham; catalog no. 17-0756). The bound protein and beads were washed three times with ice-cold NP-40 buffer (50 mM Tris-Cl [pH 8.0], 200 mM NaCl, 1% NP-40, 4 μg/ml aprotinin, 4 μg/ml leupeptin, 4 μg/ml pepstatin, 1 mM phenylmethylsulfonyl fluoride). GST proteins were eluted from glutathione-Sepharose beads by incubation in 20 mM reduced glutathione solution containing 50 mM Tris, pH 8.0, for 5 min on ice. The beads were pelleted, and the supernatant was transferred to an equal volume of 2× Laemmli buffer and heated to 100°C for 5 min. The proteins were electrophoretically resolved on a 10% SDS-polyacrylamide gel. The gel was then incubated for 1 h in fixing solution (50% methanol [vol/vol], 10% glacial acetic acid [vol/vol]). Protein bands were visualized by colloidal Coomassie staining or Spyro Ruby. Relevant bands were excised from the gel and submitted to a core facility maintained at the Biotechnology Resource Center, Cornell University, where the incorporated protein was digested with trypsin, followed by matrix-assisted laser desorption ionization–time of flight (MALDI-TOF) mass spectrometry to determine the masses of the tryptic peptides.

Coimmunoprecipitation. Approximately 10^7 HEp-2 cells were infected with 5 PFU per cell of either wild-type HSV-1(F) or vRR1204. Sixteen hours later, the cells were lysed by gentle rocking for 1 h in 1 ml cold RIPA buffer (50 mM Tris-HCl, pH 7.4, 150 mM NaCl, 1% NP-40, 0.25% Na-deoxycholate, 1 mM EDTA) containing 1× Complete Protease Inhibitor Cocktail (Roche) and phosphatase inhibitor (10 mM NaF, 10 mM Na_3VO_4). All the following steps were performed at 4°C or on ice. Insoluble material was removed by centrifugation at 18,000 × *g*. The supernatant was then precleared by incubation with nonimmune rabbit serum and 20 μl of a slurry (approximately 50%) of Protein A/G Plus-Agarose beads (Santa Cruz Biotechnology) for 2 h. The beads were removed by centrifugation at 18,000 × *g* for 15 min. Two micrograms rabbit anti-emerin antibody (Santa Cruz Biotechnology; sc-15378) or nonimmune rabbit serum was then added to the precleared supernatants. After overnight incubation, the reaction mixture was further clarified by centrifugation for 15 min at 18,000 × *g*, and 20 μl of a slurry of Protein A/G Plus-Agarose beads was added to the supernatants for another 2-h incubation. The beads were washed three times with PBS plus 0.5% Tween 20, boiled in SDS-PAGE sample buffer (10 mM Tris-HCl, pH 8.0, 10 mM β-mercaptoethanol, 20% glycerol, 5% SDS, and trace amounts of bromophenol blue), and subjected to electrophoresis through a 12% polyacrylamide gel in the presence of 0.1% SDS. The resolved protein samples were transferred electrically to nitrocellulose sheets for immunoblotting.

Immunoblotting. Nitrocellulose sheets bearing proteins of interest were blocked in 5% nonfat milk plus 0.2% Tween 20 for at least 2 h. The membrane was probed with anti-emerin goat polyclonal antibody (Santa Cruz Biotechnology; sc-8084). Primary antibody was detected by horseradish peroxidase-conjugated bovine anti-goat secondary antibody (Santa Cruz Biotechnology). Alternatively, immunoprecipitated proteins transferred to nitrocellulose were probed with a previously described chicken polyclonal antibody directed against pUL34 (52), followed by reaction with peroxidase-conjugated bovine anti-chicken secondary antibody (Santa Cruz Biotechnology). In both cases, bound immunoglobulin was visualized by enhanced chemiluminescence (Pierce), followed by exposure to X-ray film. After the immunoprecipitated material was probed for pUL34, the blot was stripped according to the manufacturer's protocols (Pierce) and reprobed with emerin-specific rabbit polyclonal antibody (Santa Cruz biotechnology; sc-15378), followed by reaction with peroxidase-conjugated goat anti-rabbit secondary antibody (Santa Cruz Biotechnology) and detection of chemiluminescence on X-ray film.

RESULTS

Emerin and EGFP-emerin relocalize in HSV-1-infected cells. To determine whether the localization of emerin changes in response to HSV infection, Vero cells were infected for 16 h with HSV-1(F), with recombinant mutants that failed to express pUL34 and pUS3, or with corresponding homologous repair viruses. The infected cells were fixed, stained for emerin by IF, and visualized by confocal microscopy (Fig. 1). As expected, in uninfected cells, emerin localized at the nuclear rim

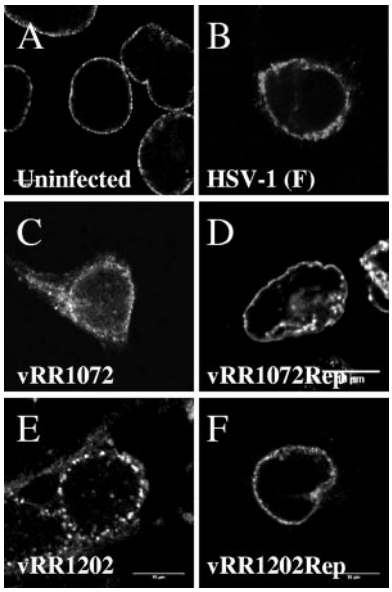

FIG. 1. Disruption of normal emerin localization in Vero cells infected with HSV-1. Shown are digital confocal images of optical sections taken near the middle of the nuclei of Vero cells fixed and stained with antibody directed against emerin. The cells were uninfected (A) or infected for 16 h with wild-type HSV-1 (B), the UL34-null recombinant vRR1072(tk+) (C), the homologous repair of vRR1072(tk+) (D), the US3-null virus vRRR1202 (E), or the homologous repair of vRR1202 (F).

with a roughly uniform distribution on the membrane (Fig. 1A). Infection with wild-type virus altered this localization. Although still concentrated at the nuclear rim, the distribution of emerin was patchier, and emerin could sometimes be seen on blebs apparently on the outer nuclear membrane (Fig. 1B). The emerin labeling of the nuclear membrane in infected cells also revealed the alterations of nuclear shape that are typical of HSV-infected cells (4, 61). Failure to express either pUL34 or pUS3 altered the localization of emerin in infected cells. In the absence of pUL34 expression, emerin no longer concentrated at the nuclear membrane and was found on both nuclear and cytoplasmic membranes (Fig. 1C). In the absence of US3 expression, emerin localized at the nuclear membrane in a punctate distribution (Fig. 1E). The local aggregates of emerin are very similar to those seen when US3-null-infected cells are stained for pUL34 (52, 53, 55). Homologous repairs of the UL34 and US3 deletions showed emerin localizations identical to that seen in cells infected with wild-type virus (Fig. 1D and F).

In US3-null infections, pUL34 adopts a punctate distribution in the nuclear membrane, and the sites of pUL34 accumulation correspond to areas of the membrane not associated with lamin proteins. The similarity of emerin aggregates and pUL34 aggregates seen in US3-null-infected cells led us to ask whether pUL34 and emerin colocalize in cells infected with wild-type virus and whether the sites of aggregation of pUL34 and of emerin in cells infected with US3-null virus might be the same. Uninfected Vero cells or cells infected for 16 h with wild-type HSV-1(F) or US3-null virus vRR1202 were stained for emerin, pUL34, and lamin A/C and visualized by confocal microscopy (Fig. 2). In cells infected with wild-type virus (Fig. 2E to H), lamin A/C, emerin, and pUL34 all colocalized ex-

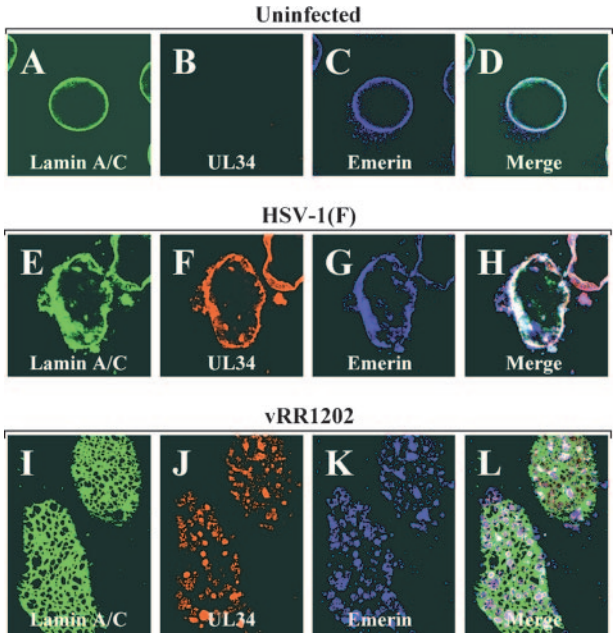

FIG. 2. Colocalization of pUL34 and emerin in cells infected with wild-type and mutant HSV-1. Shown are digital confocal images of uninfected Vero cells (A to D) or Vero cells infected with HSV-1(F) (E to H) or the US3-null virus vRR1204 (I to L) and probed for lamin A/C (green), pUL34 (red), or emerin (blue). Panels A to H show optical sections taken near the center of the cell. Panels I to L show optical sections taken at the top of the nucleus in order to visualize the perforations in the lamin network.

tensively, though areas that stained for each of the proteins individually could be seen. In cells infected with US3-null virus (Fig. 2I to L), UL34 and emerin colocalized in punctate aggregates in the nuclear membrane and the sites of costaining corresponded to areas devoid of lamin staining.

EGFP-emerin is more mobile in HSV-1-infected cells. Since emerin and lamin localizations do not separate in cells infected with wild-type HSV, connection between these proteins cannot be assessed simply by immunofluorescence. Loss of connection between the lamina and emerin would be predicted to result in greater mobility of emerin within the nuclear membrane. To test this prediction, we constructed and isolated clonal Vero cell lines that stably express EGFP-emerin fusion protein. More than 40 clonal cell lines were isolated. Proper localization of EGFP-emerin depended on the expression level of the fusion protein. Low levels of EGFP fluorescence were correlated with the tight localization to the nuclear envelope that is characteristic of endogenous emerin. Cell lines that showed intense EGFP fluorescence showed localization on cytoplasmic membranes, in addition to the nuclear envelope. Cell lines showing low-intensity EGFP fluorescence and proper emerin localization in uninfected cells were chosen for further analysis. EGFP-emerin-expressing cells were infected with wild-type, US3-null mutant, and US3 homologous repair viruses for 16 h, and the localization of the fusion protein was visualized by confocal microscopy (Fig. 3). The localization of EGFP-emerin was not distinguishable from the localization of endogenous emerin determined by immunofluorescence (compare corresponding panels of Fig. 1 and 3), demonstrating that

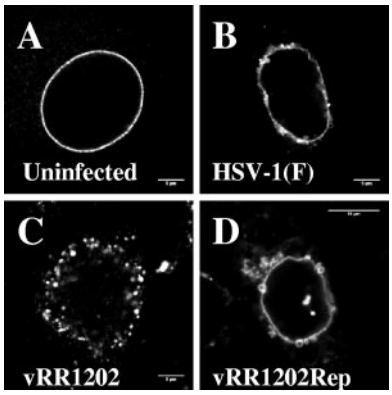

FIG. 3. EGFP-emerin localization in uninfected and infected cells. Digital confocal images of cells derived from a single clonal Vero cell line (Vero EmA) that stably expresses EGFP-emerin that were mock infected (A) or infected with wild-type HSV-1(F) (B), the US3-null virus vRR1204 (C), or the corresponding homologous repair (D) are shown. The optical sections are from the center of the nucleus.

EGFP-emerin faithfully reproduces the behavior of endogenous emerin. The behavior of EGFP-emerin in cells infected with UL34-null virus could not be assessed, since the UL34-null virus vRR1072(tk+) expresses EGFP in place of the UL34 gene.

To determine whether the mobility of EGFP-emerin changes upon infection, uninfected cells or cells infected with HSV-1(F) for 8 or 16 h were subjected to FRAP analysis, as described in Materials and Methods (Fig. 4). There was variability in fluorescence recovery among individual cells within single experiments and in recovery times between experiments, but in all experiments at both time points, data points on the early parts of the curves were significantly different ($P \leq 0.05$ using Student's t test), and at 16 h postinfection (p.i.), the mean recovery of fluorescence was roughly twice as fast in HSV-1-infected cells (half-life [$t_{1/2}$] of recovery, 39 s) as in uninfected cells. In the experiments shown, $t_{1/2}$ of recovery was 39 s for infected cells and $t_{1/2}$ of recovery was 75 s for uninfected cells.

Emerin is hyperphosphorylated in HSV-1-infected cells in a manner dependent upon UL34, US3, and PKC. To test the hypothesis that emerin is hyperphosphorylated in HSV-infected cells, HEp-2 and Vero cells were infected with HSV-1(F) for 16 h, and nuclear-lamina fractions were prepared and then reacted at 37°C in the presence or absence of CIAP. Treated samples were fractionated by SDS-PAGE, blotted to nitrocellulose, and probed for emerin (Fig. 5A). In both HEp-2 and Vero cells, emerin in uninfected cells (lanes 1 and 5) commonly appears as either a single band (as seen in this experiment) or as a doublet. Infection resulted in the appearance of slower-migrating species of emerin (lanes 3 and 7). In HEp-2 cells (lane 3), the change in migration was modest and resulted in the appearance of one or two additional species. In Vero cells (lane 7), many slower-migrating species routinely appeared. These slower-migrating species were hyperphosphorylated forms of emerin, as shown by their conversion to the single most rapidly migrating form by digestion with CIAP (lanes 4 and 8). To determine when in infection emerin becomes hyperphosphorylated, Vero cells were infected with HSV-1(F) for 4, 8, and 12 h, and lamina fractions were pre-

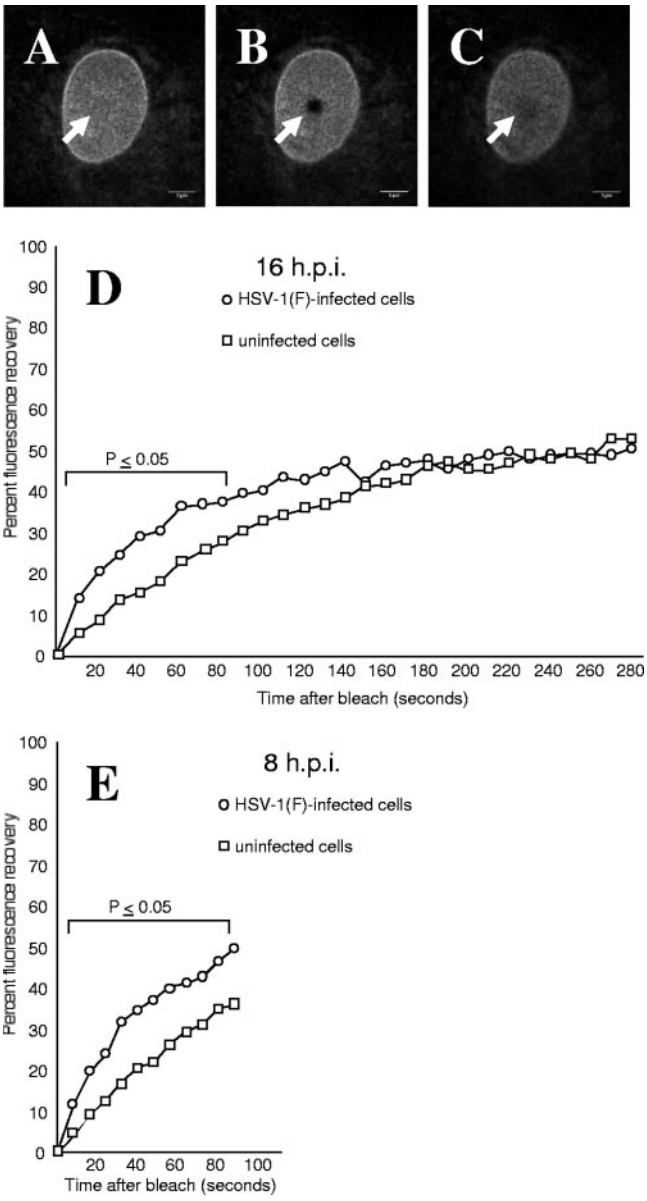

FIG. 4. FRAP analysis of EGFP-emerin in uninfected and infected cells. Live cells from clonal cell lines expressing EGFP-emerin were analyzed by FRAP as described in Materials and Methods. Optical sections at the top of the nucleus (A) were bleached by intense laser exposure (B), and recovery of fluorescence due to diffusion of unbleached molecules into the bleached region was measured (C). The arrowheads indicate the positions of the bleached areas. (D) Graph of recovery of emerin fluorescence after photobleaching at 16 h p.i. Each point represents the mean of 10 cells from one representative experiment. Statistically significant differences between points on the curves are indicated by the bracket above the curves. Three independent experiments were performed for the cell line shown (Vero EmA), and the results were reproduced with an independent clonal cell line (Vero EmAJ). (E) The same as D, except FRAP analysis was performed at 8 h p.i.

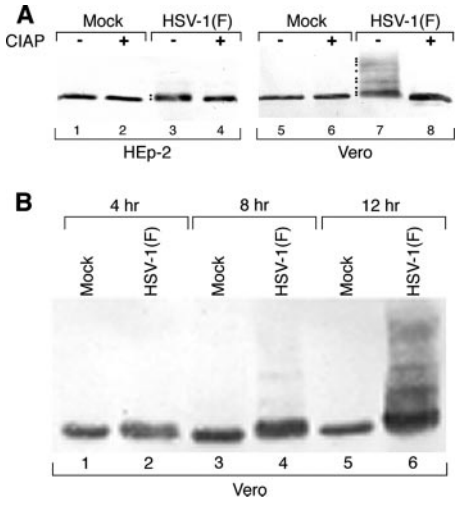

FIG. 5. Hyperphosphorylation of emerin in HSV-1-infected cells. Shown is a digital image of a Western blot of lamina fractions of HEp-2 or Vero cells that were mock infected or infected with 5 PFU/cell of HSV-1(F). (A) Cells were mock infected or infected for 16 h with 5 PFU/cell of HSV-1(F). Lamina fractions were then left untreated or treated with CIAP. The blot was probed with monoclonal antibody specific for emerin. Hyperphosphorylated species of emerin are indicated with dots to the left of the lane. (B) Vero cells were mock infected or infected for 4, 8, and 12 h with 5 PFU/cell of HSV-1(F). Lamina fractions were separated by SDS-PAGE, blotted, and probed for emerin.

pared, fractionated by SDS-PAGE, blotted to nitrocellulose, and probed for emerin (Fig. 5B). Hyperphosphorylation of emerin appears to occur in two phases. Limited hyperphosphorylation of emerin is detectable as early as 4 p.i. (lane 2) and is maintained to at least 8 h p.i. (lane 4), and extensive hyperphosphorylation is evident by 12 h p.i. (lane 6).

Two of the components of the envelopment machinery bring kinase activity to the nuclear membrane that might be responsible for emerin hyperphosphorylation. US3 has an intrinsic kinase activity, and pUL34 has been shown to recruit PKCδ and PKCα isoforms to the nuclear membrane (48). To determine whether pUL34 and pUS3 are necessary for emerin hyperphosphorylation, Vero and HEp-2 cells were infected with wild-type HSV-1(F), recombinant mutant viruses that fail to express pUS3 (vRR1202) or pUL34 (vRR1072), a virus that expresses catalytically inactive pUS3 (vRR1204), and corresponding homologous repair viruses. Nuclear-lamina fractions were prepared, separated on SDS-PAGE gels, and probed for emerin (Fig. 6). In both Vero cells (Fig. 6A) and HEp-2 cells (Fig. 6B), failure to express either pUL34 (Fig. 6A, lane 8, and B, lane 6) or pUS3 (Fig. 6A and B, lanes 3) or expression of catalytically inactive pUS3 (Fig. 6A and B, lanes 5) resulted in a change in the migration pattern of emerin such that faster-migrating species appeared. In the case of Vero cells infected with US3-null and catalytically inactive US3 viruses (Fig. 6A, lanes 3 and 5), some of the emerin migrates at the same position as emerin in uninfected cells (lane 1). In HEp-2 cells infected with either UL34-null (Fig. 6B, lane 6) or US3-null (Fig. 6B lane 3) virus or catalytically inactive US3 virus (Fig. 6B, lane 5), the migration of emerin failed to return to that in mock-infected cells, and the patterns of emerin species differed between UL34-null-infected cells and cells infected with either of the US3 mutant viruses. These results show that the hyperphosphorylation of emerin has both US3-dependent and UL34-dependent components and that either of these compo-

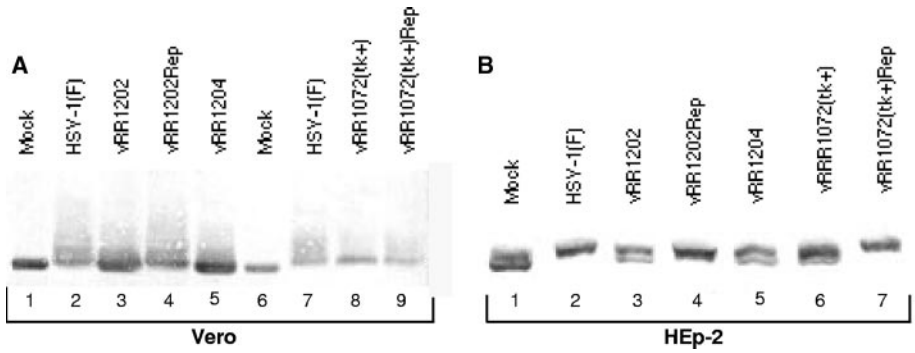

FIG. 6. Alterations in modifications of emerin in cells infected with HSV-1 mutants. Shown are digital images of Western blots of lamina fractions of Vero (A) or HEp-2 (B) cells that had been infected at 5 PFU/cell for 16 h with wild-type HSV-1(F) (panel A, lanes 2 and 7; panel B, lane 2), US3-null virus vRR1202 (panel A, lane 3, and panel B, lane 3), homologous repair of vRR1202 (panel A, lane 4; panel B, lane 4), recombinant virus expressing catalytically inactive US3 vRR1204 (panel A, lane 5; panel B, lane 5), UL34-null virus vRR1072(tk+) (panel A, lane 8; panel B, lane 6), and homologous repair of vRR1072(tk+) (panel A, lane 9; panel B, lane 7). The blots were probed with monoclonal antibody to emerin.

nents can modify infected-cell emerin to some degree. This result suggests the hypothesis that the UL34- and US3-dependent components combined might account for the total emerin hyperphosphorylation.

Since UL34 recruits PKCδ and PKCα isoforms to the nuclear membrane, we hypothesized that these kinases might be responsible for the US3-independent, UL34-dependent component of emerin hyperphosphorylation. To test this hypothesis, HEp-2 and Vero cells were infected with wild-type HSV-1(F) or recombinant US3-null virus and treated with the PKCδ-specific inhibitor rottlerin, the PKCα-specific inhibitor RO-31-7549, or both inhibitors. Nuclear-lamina fractions were analyzed by Western blotting (Fig. 7). Treatment of wild-type-infected Vero (Fig. 7A) or HEp-2 (Fig. 7B) cells with rottlerin alone (lanes 4 to 6) resulted in some loss of hyperphosphorylation, as indicated by a shift to more rapidly migrating emerin species, but did not return emerin migration to the level in mock-infected cells. This result suggests that PKCδ is responsible for some, but not all, emerin hyperphosphorylation. Treatment of either cell line with RO-31-7549 alone (Fig. 7A and B, lanes 13 to 15) did not produce any apparent shift in emerin migration compared to cells treated with vehicle alone (Fig. 7A and B, lanes 10 to 12), suggesting that PKCα does not contribute significantly to emerin phosphorylation. Treatment of US3-null-infected cells with rottlerin (Fig. 7A and B, lane 6) converted all of the emerin to the uninfected-cell form, suggesting that emerin hyperphosphorylation is the result of the combined actions of US3 and PKCδ. To test the hypothesis that the UL34-dependent and PKCδ-dependent components of emerin hyperphosphorylation are the same, Vero cells were infected with wild-type, UL34-null, and homologous repair virus with or without rottlerin treatment, and nuclear-lamina fractions were analyzed by Western blotting (Fig. 7C). While treatment with rottlerin dramatically decreased emerin hyperphosphorylation in cells infected with wild-type or repair virus (Fig. 7, compare lanes 3 and 4 with lanes 7 and 8), we observed no significant difference in the degree of hyperphosphorylation seen in cells infected with UL34-null virus (compare lanes 2 and 6). This result suggests that the UL34-dependent component of emerin phosphorylation is mediated by PKCδ.

pUL34 and emerin interact in vitro and in the infected cell. In order to identify proteins that interact with pUL34, the UL34 open reading frame was fused to the C terminus of the gene encoding GST, and the resulting fusion protein was purified from lysates of *Escherichia coli* by affinity chromatography on glutathione-Sepharose beads. As a control, GST was purified similarly. The beads bearing GST or the GST-pUL34 fusion protein were reacted with uninfected cell lysates, and proteins bound to the beads after extensive washing were eluted in reduced glutathione and electrophoretically separated on denaturing polyacrylamide gels (Fig. 8A).

After being stained, a band containing protein with an apparent M_r of around 35,000 was readily visible in lanes corresponding to the GST-pUL34 pull-down reaction but was absent from the control GST pull down. This band was not a breakdown product of GST-pUL34, inasmuch as it was not present in the purified fusion protein preparation that was reacted with PBS (Fig. 8A, lane 3). The band was therefore excised and subjected to digestion with trypsin and analysis by MALDI-TOF mass spectrometry. The masses of the resultant peptides were subjected to a homology search against the human, viral, and *E. coli* databases using Mascot software. Of the tryptic peptides with masses different from those predicted from digestion of GST or pUL34, six matched predicted tryptic peptides from four separate regions of human emerin. The masses of these peptides and the predicted masses of corresponding peptides of emerin are shown in Table 1. We conclude that emerin interacts with the GST-pUL34 fusion protein but not with GST alone.

To confirm the possibility that emerin interacted with pUL34, the pull down as described above was repeated. As a control, Hep2 cell lysates that had not been subjected to the pull-down reaction were separated on a separate lane. Proteins bound to GST and GST-pUL34 were electrophoretically separated, transferred to nitrocellulose, and probed with antibody directed against emerin, as indicated in Materials and Methods. As shown in Fig. 8B, the lysate contained ample amounts of emerin (lane 1). More importantly, emerin was detected in the GST-pUL34 pull-down reaction, but not in the GST pull-down reaction.

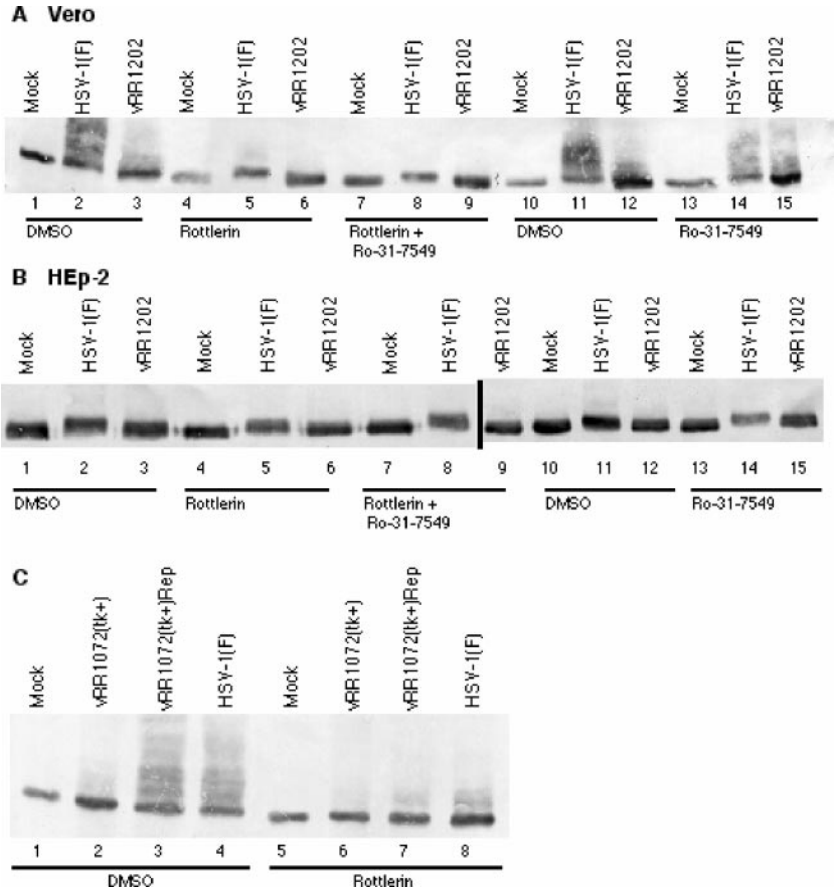

FIG. 7. Role of PKC in emerin modification. (A and B) Digital images of Western blots of lamina fractions of mock-infected, HSV-1(F)-infected, or US3-null (vRR1202)-infected Vero (A) or HEp-2 (B) cells probed for emerin. The cells were treated with the PKCδ isoform inhibitor rottlerin beginning at 5 h p.i. (lanes 4 to 9), the PKCα isoform inhibitor Ro-31-7549 beginning at 13 h p.i. (lanes 7 to 9 and 13 to 15), or vehicle (dimethyl sulfoxide) (lanes 1 to 3 and 10 to 12). The cells were maintained in the presence of inhibitors until 16 h after infection, when the cells were harvested and nuclear-lamina fractions were prepared. The times chosen for exposure to inhibitor were determined in pilot experiments to give maximal effect. In panel B, all samples are from the same experiment, but lanes 1 to 8 and lanes 9 to 15 are from separate gels. (C) Digital image of a Western blot of lamina fractions of mock-infected, HSV-1(F)-infected, or UL34-null-infected Vero cells probed for emerin. The cells were treated with rottlerin as described for panels A and B.

To further confirm the emerin-pUL34 interaction, document the reciprocal interaction, and show that the interaction occurs in HSV-infected cells, cells were infected with HSV-1(F) and the catalytically inactive US3 (K220A) virus vRR1204. Lysates of these cells were subjected to immunoprecipitation with nonimmune antibody or an emerin-specific antibody. Purified antigen-antibody complexes were eluted in SDS, and immunoblots of the reaction components were probed with antibodies directed against pUL34 and emerin. As shown in Fig. 8C, while there was some background immunoreactivity that was immunoprecipitated with nonimmune serum, the emerin-specific antibody greatly enhanced the amount of coimmunoprecipitated emerin and pUL34. Moreover, pUL34 and emerin were coimmunoprecipitated from lysates of cells infected with either HSV-1(F) or vRR1204. These data confirm the GST pull-down reactions described above using uninfected cell lysates and, consistent with the above data, indicate that the emerin-pUL34 interaction can occur in the presence or absence of US3 kinase activity.

Emerin expression is not necessary for productive infection. To test the hypothesis that emerin is required for viral growth, parallel cultures of MEFs derived from wild-type ($MEF^{+/y}$) and emerin-null ($EM^{-/y}$) mice were infected with 5 PFU/cell of HSV-1(F) and production of virus infectivity was measured at various times after infection (Fig. 9). Similar levels of infectivity were produced by $MEF^{+/y}$ and $EM^{-/y}$ fibroblasts at all times after infection, indicating that the expression of emerin is not essential for viral growth.

Capsids are not required for infection-dependent changes in nuclear shape and emerin localization. The infection-dependent changes seen in nuclear shape, lamin organization, and emerin localization could be explained in two ways. These changes might reflect disruptions of the lamina that are carried out prior to and are necessary for nuclear-capsid envelopment. It is also possible that these changes are secondary to capsid envelopment (i.e., the act of budding of large numbers of capsids through the nuclear envelope results in substantial changes in the organization of envelope components). In order

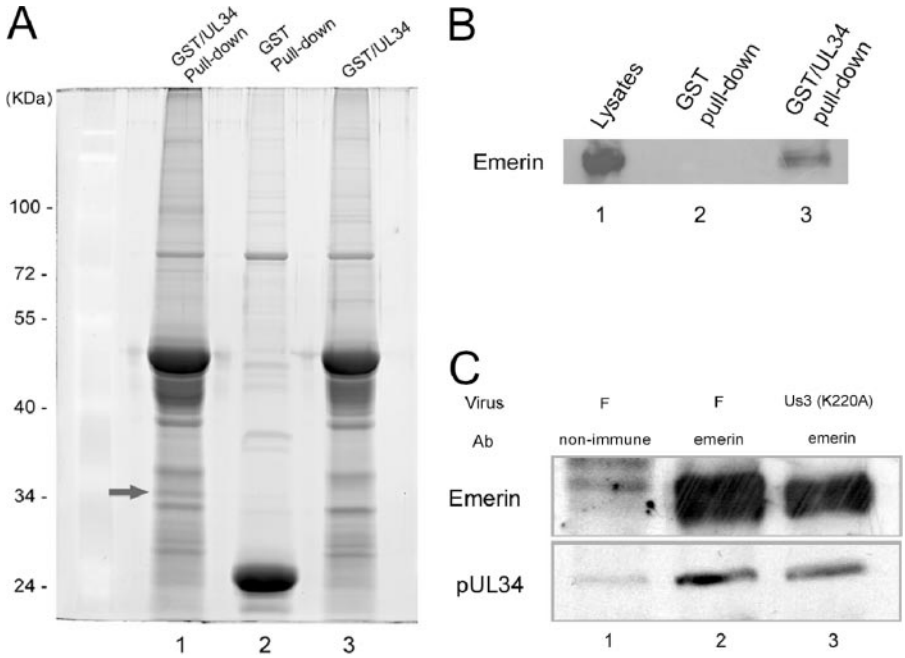

FIG. 8. Interaction between emerin and pUL34. (A) Spyro Ruby-stained SDS-polyacrylamide gel of pUL34-GST pull down. GST (lane 2) or a fusion protein containing full-length pUL34 fused to GST was purified by affinity chromatography on glutathione-Sepharose beads and, while on the beads, was reacted with PBS (lane 3) or a clarified lysate of HEp-2 cells (lanes 1 and 2). The arrow indicates a protein band specifically pulled down by GST-pUL34 but not by GST. This band was excised and determined to contain emerin by MALDI-TOF mass spectrometry of the tryptic peptides (Table 1). The masses of the standards (in thousands) are indicated on the left. (B) Immunoblot probed with antibody to emerin. HEp-2 cell lysates (lane 1) or proteins bound to glutathione-conjugated Sepharose beads bearing GST (lane 2) or a GST-UL34 fusion protein (lane 3) were eluted in SDS, electrophoretically separated on a denaturing gel, transferred to nitrocellulose, and probed with goat anti-emerin antibody, followed by reaction with horseradish peroxidase-conjugated anti-goat antibody, addition of enhanced-chemiluminescence fluorogenic substrate (Amerhsham), and exposure to X-ray film. (C) Immunoprecipitation of emerin, followed by immunoblotting with pUL34 and emerin-specific antibodies. Lysates of HEp-2 cells infected with HSV-1(F) (lanes 1 and 2) or an HSV-1(F) mutant bearing a mutation that precludes US3 kinase activity (lane 3) were subjected to immunoprecipitation with rabbit anti-emerin antibody (lanes 1 and 3) or nonimmune serum (lane 1). Immunoprecipitated proteins were electrophoretically separated and subjected to immunoblotting with emerin-specific (top) or pUL34-specific (bottom) antibody. Bound IgG was identified as in panel B, except that the secondary antibodies were horseradish peroxidase-conjugated goat anti-rabbit and anti-chicken for the upper and lower blots, respectively.

to distinguish between these possibilities, Vero cells were infected for 16 h with either HSV-1(F) or recombinant virus that failed to express the major capsid protein VP5, fixed, and processed for confocal immunofluorescence microscopy using antibodies directed against UL34, lamin A/C, or emerin (Fig. 10). Nuclei of cells infected with both wild-type and VP5-null

TABLE 1. Parameters of experimental and emerin-specific tryptic peptides

Observed ratio[a]	M_r		Peptide[d]
	Experimental[b]	Calculated[c]	
471.37	940.72	940.47	APGAGLGQDR
543.37	1,084.73	1,084.52	IFEYETQR
414.79	1,241.35	1,240.62	IFEYETQRR
625.86	1,249.71	1,249.56	TYGEPESAGPSR
625.88	1,249.74	1,249.56	TYGEPESAGPSR
466.38	1,396.11	1,395.73	YNIPHGPVVGSTR
518.42	1,552.22	1,551.83	RYNIPHGPVVGSTR

[a] Mass-to-charge ratio (m/z) of experimental peptide.
[b] Calculated M_r of experimental tryptic peptide.
[c] Calculated M_r of emerin peptide from database.
[d] Amino acid sequence of matching peptide in single-letter code.

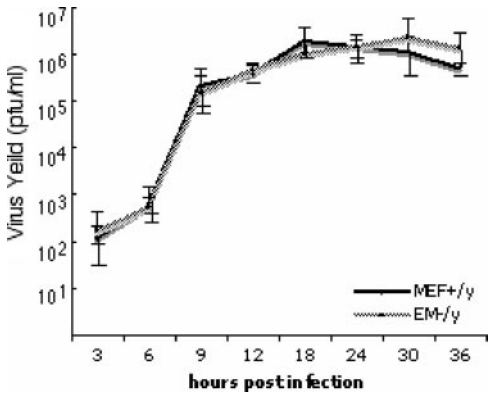

FIG. 9. Emerin is not required for HSV-1(F) replication. Replicate cultures of wild-type MEFs ($MEF^{+/y}$) and emerin-null MEFs ($EM^{-/y}$) were infected at a multiplicity of infection of 5 with HSV-1(F). Residual virus was removed or inactivated with a low-pH wash, and at the indicated times, total-culture virus was titrated on Vero cells. Virus yields are expressed as PFU per milliliter. Each data point represents the mean of three independent experiments. The error bars indicate simple standard deviations.

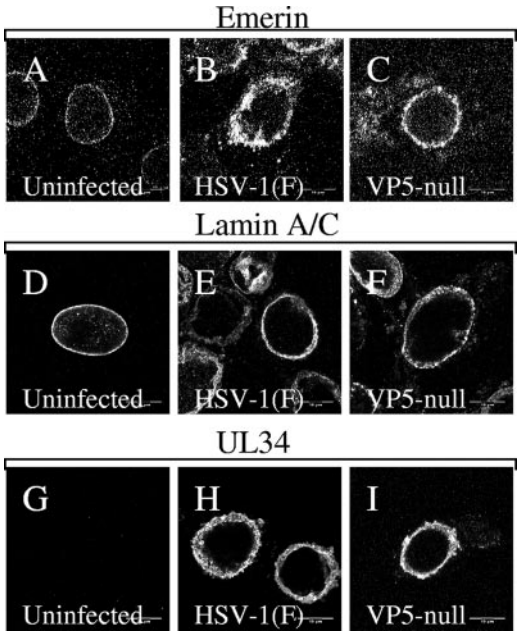

FIG. 10. Localization of emerin, lamin A/C, and pUL34 in cells infected with VP5-null virus. Digital confocal images of Vero cells that were uninfected (A, D, and G) or infected with wild-type HSV-1(F) (B, E, and H) or a VP5-null recombinant virus (C, F, and I) are shown. Fixed cells were reacted with antibody to emerin (A to C), lamin A/C (D to F), or pUL34 (G to H). The optical sections were taken near the center of the nucleus.

viruses are irregularly shaped to similar degrees (compare Fig. 10A, B, and C), show uneven distribution of lamin A/C (Fig. 10E and F), and show similar changes in the localization of emerin (Fig. 10B and C). These results suggest that envelopment of capsids is not responsible for the observed changes in the organization of nuclear-lamina components.

DISCUSSION

Emerin is mobilized from the inner nuclear membrane during HSV-1 infection. The localization of emerin changes so that, rather than evenly lining the nuclear membrane, it shows an uneven distribution with concentrations on blebs that appear to be on the outer surface of the nuclear membrane. In cells infected with US3-null virus, emerin no longer localizes with lamins at all, and in cells infected with UL34-null virus, much of it is no longer associated with the nuclear membrane, suggesting that under these conditions it has lost any binding connections to the lamin proteins. It is more difficult to assess connection between the lamins and emerin in cells infected with wild-type virus, since both proteins are still colocalized and associated with the nuclear membrane. FRAP analysis, which can assess the mobility and consequently the "connectedness" of proteins, suggests that emerin is less tightly coupled to an immobile nuclear lamina.

That phosphorylation of emerin is tied to its function is shown by several lines of evidence. Emerin is phosphorylated in a cell cycle-dependent manner. Emerin may be phosphorylated at all phases of the cell cycle, but the greatest degree of phosphorylation is observed in M phase (13), leading to the suggestion that phosphorylation of emerin is responsible for its dissociation from the lamina during disassembly of the nucleus in preparation for mitosis. Emerin is aberrantly hyperphosphorylated in cells from some EDMD patients, suggesting that such aberrant phosphorylation of emerin can contribute to EDMD pathogenesis (13).

Emerin is hyperphosphorylated in HSV-1-infected cells, as shown by decreased mobility of emerin and greater heterogeneity of mobility in SDS-PAGE gels and the complete reversibility of the changes in mobility by treatment with phosphatase. Interestingly, in both Vero and HEp-2 cells, all emerin detected by Western blotting runs more slowly in SDS-PAGE than emerin from uninfected cells, suggesting that the entire emerin population is hyperphosphorylated to at least some degree in infected cells. Changes in lamin B and lamin A/C localization in infected cells are consistent with limited and localized disruption of the integrity of the lamina. Global hyperphosphorylation of emerin and the increased mobility of emerin in the nuclear envelope, on the other hand, suggest that the loss of emerin-lamin connections may occur all over the inner nuclear membrane. The difference in the degree of emerin hyperphosphorylation between Vero and HEp-2 cells is quite dramatic, but its functional consequences are not clear. Although we have measured emerin mobility using FRAP only in Vero cell lines, observation of emerin relocalization in HEp-2 cells infected with wild-type and UL34 and US3 mutant viruses shows no difference from Vero cells (not shown). These observations do not, however, address changes in functions of emerin other than its localization, and these functions may be regulated differently in HEp-2 and Vero cells.

Failure of HSV-1 to express either pUS3 or pUL34 results in failure to normally hyperphosphorylate emerin (Fig. 6). The migration of hyperphosphorylated species differs depending on whether pUL34 or pUS3 is missing, suggesting that each viral protein makes an independent contribution to emerin hyperphosphorylation. Studies in a *Xenopus* oocyte cell-free system show M-phase phosphorylation of emerin on five residues (23). The phosphorylated serine nearest the LEM domain (S49) is in a perfect US3 phosphorylation consensus, raising the possibility that pUS3 contributes to emerin hyperphosphorylation and disconnection from the lamina by direct phosphorylation of this site.

HSV-1 pUL34 has been shown to mediate recruitment of PKC isoforms to the nuclear membrane in infected cells (48). Both PKCα and PKCδ were relocalized to the nuclear membrane in a manner dependent upon both pUL34 and pUL31 and in a manner independent of pUS3. The dependence of emerin hyperphosphorylation upon pUL34 and its sensitivity to rottlerin suggest that the UL34-dependent component of emerin hyperphosphorylation may reflect pUL34/pUL31-dependent recruitment of PKCδ to the nuclear membrane.

PKC is a family of serine/threonine kinases that are involved in regulation of cellular processes, including growth, migration, and inflammatory responses. PKCδ is a calcium-independent, or novel, PKC isoform whose activity is regulated by a variety of different factors, including oxidative stress, UV exposure, and inflammatory cytokines. PKCδ has been implicated as a regulator of cell proliferation and as a critical mediator of apoptosis in some cell types (5, 27). No role has been proposed for PKCδ in nuclear-envelope breakdown or assembly, and it is

clearly not uniquely required for nuclear-lamina disassembly in cell division, since PKCδ$^{-/-}$ mice are viable. PKCδ can, however, be recruited for phosphorylation of lamin B during apoptosis. PKCδ knockout mice are impaired in their ability to control B-cell proliferation and B-cell-mediated autoimmunity, and they show enhanced development of arteriosclerosis in vein grafts and impaired ability to undergo apoptosis in response to a variety of stimuli (38, 41). Substrate specificity of PKC isoforms is thought to be conferred in large part by recruitment of active enzyme to the site of the substrate. In uninfected cells, recruitment of PKC isoforms to specific subcellular locations is accomplished by RACKs and other PKC-interacting proteins that bind specifically to activated forms of PKC (42, 50). It may be that pUL34 or pUL31, or the complex of these two proteins, functions as a RACK for PKCδ.

Interestingly, neither the pUL34-dependent nor the pUS3-dependent components of emerin hyperphosphorylation are uniquely required in order to disrupt the connection between emerin and lamins. The complete loss of colocalization of emerin and lamins in cells infected with US3-null virus shows that loss of connection can occur in the absence of US3 expression. The relocalization of a large fraction of cellular emerin to cytoplasmic membranes in cells infected with UL34-null virus suggests that loss of emerin-lamin connections can also occur in the absence of pUL34 expression.

The physical interaction between pUL34 and emerin provides an explanation for colocalization of pUL34 and emerin in cells infected with wild-type and US3-null viruses. In the absence of pUL34, emerin is mobilized to cytoplasmic membranes, suggesting that in a cell infected with wild-type virus, emerin is retained in the nuclear envelope, despite its loss of connection to the lamina, by its interaction with pUL34.

Our results are consistent with a model in which increased emerin mobility and relocalization in infected cells results from hyperphosphorylation of emerin. This hyperphosphorylation has UL34- and US3-dependent components. The UL34-dependent component is mediated by UL34-recruited PKCδ and -α isoforms, and perhaps to some degree by US3 recruited to the nuclear envelope. There is also a UL34-independent component of emerin hyperphosphorylation that may result wholly, or in part, from US3-mediated phosphorylation of emerin that occurs even in the absence of UL34. Either pUL34- or pUS3-dependent hyperphosphorylation is sufficient to loosen emerin-lamin connections. Emerin is nonetheless retained in the nuclear envelope by virtue of its physical interaction with pUL34.

The changes in emerin localization shown in this paper, and the changes in the nuclear shape and distribution of lamin proteins, are not dependent on ongoing capsid envelopment, since they occur in cells infected with a virus that cannot make capsids due to a deletion of the gene encoding the major capsid protein (Fig. 10). This suggests that infection-dependent alterations of the nuclear envelope may occur in preparation for capsid envelopment, rather than as a result of it. Klupp et al. have recently demonstrated formation of UL31- and UL34-containing vesicles from the inner nuclear membranes of cells that coexpress these proteins in the absence of other viral factors (31). These results suggest that, in addition to disruption of the nuclear lamina, other facets of the envelopment reaction may occur in the absence of capsids under appropriate conditions.

Alphaherpesvirus US3 homologs have been implicated in diverse processes in infected cells, including inhibition of apoptosis, de-envelopment of capsids at the outer nuclear membrane, and rearrangement of the actin cytoskeleton. Although pUL34 was the first identified substrate of the US3 protein kinase activity, it is now clear that there are probably many others. For example, the viral UL31, US9, and ICP22 proteins can be directly phosphorylated by US3 (29), and lamin A/C is a cellular substrate for US3 activity (44). It is not yet clear whether and to what degree phosphorylation of these substrates affects replication of HSV in culture or in vivo. The US3 envelopment function is reflected in two related phenotypes of a US3-null virus: (i) change in distribution of pUL34 and pUL31 in the nuclear membrane from the roughly continuous distribution seen in wild-type-infected cells to distribution in discrete aggregates, as seen in Fig. 2A; (ii) accumulation of enveloped virus particles in distensions of the perinuclear space due to inhibition of de-envelopment. These accumulations of virus particles correspond to the sites of pUL34 and pUL31 localization, apparently because pUL34 and pUL31 are structural components of the enveloped perinuclear virions. pUS3 is a substrate for the protein kinase encoded by the UL13 gene, and this phosphorylation is necessary for the pUS3 envelopment function (30). If emerin hyperphosphorylation is a critical element of that function, then it, too, should require expression of pUL13.

We began these studies guided by the hypothesis that emerin, as a component of the nuclear lamina, represented a problem for HSV-1 replication. Our results, however, are consistent with other interesting possibilities. The concentrations of pUL34 in US3-null-infected cells correspond to accumulations of perinuclear virions that are labeled heavily with UL34 antibody in immunogold localization experiments (32, 53). The interaction of emerin with pUL34 and the colocalization of emerin with pUL34 in US3-null-infected cells suggests the hypothesis that emerin, like pUL34, may also be a structural component of the perinuclear virion. However, unlike pUL34, emerin is clearly not an essential cofactor for virus assembly, since HSV can replicate efficiently in cells that do not express emerin. In addition to its role in assembly and maintenance of nuclear-lamina structure, roles have been proposed for emerin in the organization of nuclear actin and in regulation of gene expression (17, 20, 24, 25, 64). It is possible that HSV-mediated hyperphosphorylation of emerin regulates one or more of these functions of emerin to enhance virus replication and spread in the human host.

Hyperphosphorylation of emerin in HSV-infected cells has recently been reported by Morris et al. (43). These authors observe that hyperphosphorylation is correlated with greater extractability of emerin, which is consistent with our finding that emerin mobility in the nuclear membrane is increased. These authors found that emerin hyperphosphorylation depended upon US3 in HSV-2-infected cells and that it could be inhibited by an inhibitor of the cyclin-dependent kinase CDK1. The dependence on CDK1 activity is interesting, since inhibitors of CDKs, including CDK1, inhibit multiple steps in the virus life cycle (8, 11, 28, 56–58), and a dominant-negative CDK1 inhibits viral-DNA replication and late-gene expression

(1). CDK1 inhibition may depress expression of late genes, and the CDK1 dependence of emerin phosphorylation may reflect lower UL34 expression and recruitment of PKCδ.

ACKNOWLEDGMENTS

We thank Prashant Desai for the kind gift of the VP5-null virus and complementing cells and Colin Stewart for the gift of wild-type and emerin-null fibroblasts. We also thank the staff of the Central Microscopy Research Facility of the University of Iowa, and especially Tom Moninger, for expertise and help with confocal microscopy and FRAP analysis and Sheng Zhang at the Cornell Biotechnology Resource Center for advice on mass spectrometry.

These studies were supported by the University of Iowa and Public Health Service awards AI 41478 to R.J.R. and AI 52341 to J.B.

REFERENCES

1. **Advani, S. J., R. R. Weichselbaum, and B. Roizman.** 2001. cdc2 cyclin-dependent kinase binds and phosphorylates herpes simplex virus 1 U_L42 DNA synthesis processivity factor. J. Virol. **75:**10326–10333.
2. **Aebi, U., J. Cohn, L. Buhle, and L. Gerace.** 1986. The nuclear lamina is a meshwork of intermediate-type filaments. Nature **323:**560–564.
3. **Bione, S., E. Maestrini, S. Rivella, M. Mancini, S. Regis, G. Romeo, and D. Toniolo.** 1994. Identification of a novel X-linked gene responsible for Emery-Dreifuss muscular dystrophy. Nat. Genet. **8:**323–327.
4. **Bjerke, S. L., and R. Roller.** 2006. Roles for herpes simplex type 1 UL34 and US3 proteins in disrupting the nuclear lamina during herpes simplex virus type 1 egress. Virology **76:**261–276.
5. **Brodie, C., and P. M. Blumberg.** 2003. Regulation of cell apoptosis by protein kinase C delta. Apoptosis **8:**19–27.
6. **Clements, L., S. Manilal, D. R. Love, and G. E. Morris.** 2000. Direct interaction between emerin and lamin A. Biochem. Biophys. Res. Commun. **267:**709–714.
7. **Courvalin, J. C., N. Segil, G. Blobel, and H. J. Worman.** 1992. The lamin B receptor of the inner nuclear membrane undergoes mitosis-specific phosphorylation and is a substrate for p34cdc2-type protein kinase. J. Biol. Chem. **267:**19035–19038.
8. **Davido, D. J., W. F. Von Zagorski, G. G. Maul, and P. A. Schaffer.** 2003. The differential requirement for cyclin-dependent kinase activities distinguishes two functions of herpes simplex virus type 1 ICP0. J. Virol. **77:**12603–12616.
9. **Dechat, T., J. Gotzmann, A. Stockinger, C. A. Harris, M. A. Talle, J. J. Siekierka, and R. Foisner.** 1998. Detergent-salt resistance of LAP2α in interphase nuclei and phosphorylation-dependent association with chromosomes early in nuclear assembly implies functions in nuclear structure dynamics. EMBO J. **17:**4887–4902.
10. **Desai, P., N. A. DeLuca, J. C. Glorioso, and S. Person.** 1993. Mutations in herpes simplex virus type 1 genes encoding VP5 and VP23 abrogate capsid formation and cleavage of replicated DNA. J. Virol. **67:**1357–1364.
11. **Diwan, P., J. J. Lacasse, and L. M. Schang.** 2004. Roscovitine inhibits activation of promoters in herpes simplex virus type 1 genomes independently of promoter-specific factors. J. Virol. **78:**9352–9365.
12. **Dreger, M., H. Otto, G. Neubauer, M. Mann, and F. Hucho.** 1999. Identification of phosphorylation sites in native lamina-associated polypeptide 2 beta. Biochemistry **38:**9426–9434.
13. **Ellis, J. A., M. Craxton, J. R. Yates, and J. Kendrick-Jones.** 1998. Aberrant intracellular targeting and cell cycle-dependent phosphorylation of emerin contribute to the Emery-Dreifuss muscular dystrophy phenotype. J. Cell Sci. **111:**781–792.
14. **Fairley, E. A., J. Kendrick-Jones, and J. A. Ellis.** 1999. The Emery-Dreifuss muscular dystrophy phenotype arises from aberrant targeting and binding of emerin at the inner nuclear membrane. J. Cell Sci. **112:**2571–2582.
15. **Farina, A., R. Feederle, S. Raffa, R. Gonnella, R. Santarelli, L. Frati, A. Angeloni, M. R. Torrisi, A. Faggioni, and H. J. Delecluse.** 2005. BFRF1 of Epstein-Barr virus is essential for efficient primary viral envelopment and egress. J. Virol. **79:**3703–3712.
16. **Foisner, R., and L. Gerace.** 1993. Integral membrane proteins of the nuclear envelope interact with lamins and chromosomes, and binding is modulated by mitotic phosphorylation. Cell **73:**1267–1279.
17. **Frock, R. L., B. A. Kudlow, A. M. Evans, S. A. Jameson, S. D. Hauschka, and B. K. Kennedy.** 2006. Lamin A/C and emerin are critical for skeletal muscle satellite cell differentiation. Genes Dev. **20:**486–500.
18. **Fuchs, W., B. G. Klupp, H. Granzow, N. Osterrieder, and T. C. Mettenleiter.** 2002. The interacting UL31 and UL34 gene products of pseudorabies virus are involved in egress from the host-cell nucleus and represent components of primary enveloped but not mature virions. J. Virol. **76:**364–378.
19. **Gruenbaum, Y., A. Margalit, R. D. Goldman, D. K. Shumaker, and K. L. Wilson.** 2005. The nuclear lamina comes of age. Nat. Rev. Mol. Cell. Biol. **6:**21–31.
20. **Haraguchi, T., J. M. Holaska, M. Yamane, T. Koujin, N. Hashiguchi, C. Mori, K. L. Wilson, and Y. Hiraoka.** 2004. Emerin binding to Btf, a death-promoting transcriptional repressor, is disrupted by a missense mutation that causes Emery-Dreifuss muscular dystrophy. Eur. J. Biochem. **271:**1035–1045.
21. **Haraguchi, T., T. Koujin, M. Segura-Totten, K. K. Lee, Y. Matsuoka, Y. Yoneda, K. L. Wilson, and Y. Hiraoka.** 2001. BAF is required for emerin assembly into the reforming nuclear envelope. J. Cell Sci. **114:**4575–4585.
22. **Heald, R., and F. McKeon.** 1990. Mutations of phosphorylation sites in lamin A that prevent nuclear lamina disassembly in mitosis. Cell **61:**579–589.
23. **Hirano, Y., M. Segawa, F. S. Ouchi, Y. Yamakawa, K. Furukawa, K. Takeyasu, and T. Horigome.** 2005. Dissociation of emerin from barrier-to-autointegration factor is regulated through mitotic phosphorylation of emerin in a *Xenopus* egg cell-free system. J. Biol. Chem. **280:**39925–39933.
24. **Holaska, J. M., A. K. Kowalski, and K. L. Wilson.** 2004. Emerin caps the pointed end of actin filaments: evidence for an actin cortical network at the nuclear inner membrane. PLoS Biol. **2:**e231.
25. **Holaska, J. M., K. K. Lee, A. K. Kowalski, and K. L. Wilson.** 2003. Transcriptional repressor germ cell-less (GCL) and barrier to autointegration factor (BAF) compete for binding to emerin in vitro. J. Biol. Chem. **278:**6969–6975.
26. **Holmer, L., and H. J. Worman.** 2001. Inner nuclear membrane proteins: functions and targeting. Cell. Mol. Life Sci. **58:**1741–1747.
27. **Jackson, D. N., and D. A. Foster.** 2004. The enigmatic protein kinase Cδ: complex roles in cell proliferation and survival. FASEB J. **18:**627–636.
28. **Jordan, R., L. Schang, and P. A. Schaffer.** 1999. Transactivation of herpes simplex virus type 1 immediate-early gene expression by virion-associated factors is blocked by an inhibitor of cyclin-dependent protein kinases. J. Virol. **73:**8843–8847.
29. **Kato, A., M. Yamamoto, T. Ohno, H. Kodaira, Y. Nishiyama, and Y. Kawaguchi.** 2005. Identification of proteins phosphorylated directly by the Us3 protein kinase encoded by herpes simplex virus 1. J. Virol. **79:**9325–9331.
30. **Kato, A., M. Yamamoto, T. Ohno, M. Tanaka, T. Sata, Y. Nishiyama, and Y. Kawaguchi.** 2006. Herpes simplex virus 1-encoded protein kinase UL13 phosphorylates viral Us3 protein kinase and regulates nuclear localization of viral envelopment factors UL34 and UL31. J. Virol. **80:**1476–1486.
31. **Klupp, B. G., H. Granzow, W. Fuchs, G. M. Keil, S. Finke, and T. C. Mettenleiter.** 2007. Vesicle formation from the nuclear membrane is induced by coexpression of two conserved herpesvirus proteins. Proc. Natl. Acad. Sci. USA **104:**7241–7246.
32. **Klupp, B. G., H. Granzow, and T. C. Mettenleiter.** 2001. Effect of the pseudorabies virus US3 protein on nuclear membrane localization of the UL34 protein and virus egress from the nucleus. J. Gen. Virol. **82:**2363–2371.
33. **Klupp, B. G., H. Granzow, and T. C. Mettenleiter.** 2000. Primary envelopment of pseudorabies virus at the nuclear membrane requires the UL34 gene product. J. Virol. **74:**10063–10073.
34. **Krohne, G.** 2004. Lamins. Methods Cell Biol. **78:**573–596.
35. **Lake, C. M., and L. M. Hutt-Fletcher.** 2004. The Epstein-Barr virus BFRF1 and BFLF2 proteins interact and coexpression alters their cellular localization. Virology **320:**99–106.
36. **Lammerding, J., J. Hsiao, P. C. Schulze, S. Kozlov, C. L. Stewart, and R. T. Lee.** 2005. Abnormal nuclear shape and impaired mechanotransduction in emerin-deficient cells. J. Cell Biol. **170:**781–791.
37. **Lee, K. K., T. Haraguchi, R. S. Lee, T. Koujin, Y. Hiraoka, and K. L. Wilson.** 2001. Distinct functional domains in emerin bind lamin A and DNA-bridging protein BAF. J. Cell Sci. **114:**4567–4573.
38. **Leitges, M., M. Mayr, U. Braun, U. Mayr, C. Li, G. Pfister, N. Ghaffari-Tabrizi, G. Baier, Y. Hu, and Q. Xu.** 2001. Exacerbated vein graft arteriosclerosis in protein kinase Cδ-null mice. J. Clin. Investig. **108:**1505–1512.
39. **Lin, F., D. L. Blake, I. Callebaut, I. S. Skerjanc, L. Holmer, M. W. McBurney, M. Paulin-Levasseur, and H. J. Worman.** 2000. MAN1, an inner nuclear membrane protein that shares the LEM domain with lamina-associated polypeptide 2 and emerin. J. Biol. Chem. **275:**4840–4847.
40. **Melcon, G., S. Kozlov, D. A. Cutler, T. Sullivan, L. Hernandez, P. Zhao, S. Mitchell, G. Nader, M. Bakay, J. N. Rottman, E. P. Hoffman, and C. L. Stewart.** 2006. Loss of emerin at the nuclear envelope disrupts the Rb1/E2F and MyoD pathways during muscle regeneration. Hum. Mol. Genet. **15:**637–651.
41. **Miyamoto, A., K. Nakayama, H. Imaki, S. Hirose, Y. Jiang, M. Abe, T. Tsukiyama, H. Nagahama, S. Ohno, S. Hatakeyama, and K. I. Nakayama.** 2002. Increased proliferation of B cells and auto-immunity in mice lacking protein kinase Cδ. Nature **416:**865–869.
42. **Mochly-Rosen, D.** 1995. Localization of protein kinases by anchoring proteins: a theme in signal transduction. Science **268:**247–251.
43. **Morris, J. B., H. Hofemeister, and P. O'Hare.** 2007. Herpes simplex virus infection induces phosphorylation and delocalization of emerin, a key inner nuclear membrane protein. J. Virol. **81:**4429–4437.
44. **Mou, F., T. Forest, and J. D. Baines.** 2007. US3 of herpes simplex type 1 encodes a promiscuous protein kinase that phosphorylates and alters localization of lamin A/C in infected cells. J. Virol. **81:**6459–6470.
45. **Muranyi, W., J. Haas, M. Wagner, G. Krohne, and U. H. Koszinowski.** 2002. Cytomegalovirus recruitment of cellular kinases to dissolve the nuclear lamina. Science **297:**854–857.

46. **Neubauer, A., J. Rudolph, C. Brandmuller, F. T. Just, and N. Osterrieder.** 2002. The equine herpesvirus 1 UL34 gene product is involved in an early step in virus egress and can be efficiently replaced by a UL34-GFP fusion protein. Virology **300:**189–204.
47. **Ozawa, R., Y. K. Hayashi, M. Ogawa, R. Kurokawa, H. Matsumoto, S. Noguchi, I. Nonaka, and I. Nishino.** 2006. Emerin-lacking mice show minimal motor and cardiac dysfunctions with nuclear-associated vacuoles. Am. J. Pathol. **168:**907–917.
48. **Park, R., and J. Baines.** 2006. Herpes simplex virus type 1 infection induces activation and recruitment of protein kinase C to the nuclear membrane and increased phosphorylation of lamin B. J. Virol. **80:**494–504.
49. **Peter, M., J. Nakagawa, M. Doree, J. C. Labbe, and E. A. Nigg.** 1990. In vitro disassembly of the nuclear lamina and M phase-specific phosphorylation of lamins by cdc2 kinase. Cell **61:**591–602.
50. **Poole, A. W., G. Pula, I. Hers, D. Crosby, and M. L. Jones.** 2004. PKC-interacting proteins: from function to pharmacology. Trends Pharmacol. Sci. **25:**528–535.
51. **Reynolds, A., L. Liang, and J. Baines.** 2004. Conformational changes of the nuclear lamina induced by herpes simplex virus 1 requires genes U_L31 and U_L34. J. Virol. **78:**5564–5575.
52. **Reynolds, A. E., B. J. Ryckman, J. D. Baines, Y. Zhou, L. Liang, and R. J. Roller.** 2001. U_L31 and U_L34 proteins of herpes simplex virus type 1 form a complex that accumulates at the nuclear rim and is required for envelopment of nucleocapsids. J. Virol. **75:**8803–8817.
53. **Reynolds, A. E., E. G. Wills, R. J. Roller, B. J. Ryckman, and J. D. Baines.** 2002. Ultrastructural localization of the herpes simplex virus type 1 U_L31, U_L34, and U_S3 proteins suggests specific roles in primary envelopment and egress of nucleocapsids. J. Virol. **76:**8939–8952.
54. **Roller, R. J., Y. Zhou, R. Schnetzer, J. Ferguson, and D. DeSalvo.** 2000. Herpes simplex virus type 1 U_L34 gene product is required for viral envelopment. J. Virol. **74:**117–129.
55. **Ryckman, B. J., and R. J. Roller.** 2004. Herpes simplex virus type 1 primary envelopment: U_L34 protein modification and the U_S3-U_L34 catalytic relationship. J. Virol. **78:**399–412.
56. **Schang, L. M., J. Phillips, and P. A. Schaffer.** 1998. Requirement for cellular cyclin-dependent kinases in herpes simplex virus replication and transcription. J. Virol. **72:**5626–5637.
57. **Schang, L. M., A. Rosenberg, and P. A. Schaffer.** 2000. Roscovitine, a specific inhibitor of cellular cyclin-dependent kinases, inhibits herpes simplex virus DNA synthesis in the presence of viral early proteins. J. Virol. **74:**2107–2120.
58. **Schang, L. M., A. Rosenberg, and P. A. Schaffer.** 1999. Transcription of herpes simplex virus immediate-early and early genes is inhibited by roscovitine, an inhibitor specific for cellular cyclin-dependent kinases. J. Virol. **73:**2161–2172.
59. **Schnee, M., Z. Ruzsics, A. Bubeck, and U. H. Koszinowski.** 2006. Common and specific properties of herpesvirus U_L34/U_L31 protein family members revealed by protein complementation assay. J. Virol. **80:**11658–11666.
60. **Scott, E. S., and P. O'Hare.** 2001. Fate of the inner nuclear membrane protein lamin B receptor and nuclear lamins in herpes simplex virus type 1 infection. J. Virol. **75:**1818–1830.
61. **Simpson-Holley, M., J. Baines, R. Roller, and D. Knipe.** 2004. Herpes simplex virus 1 $UL_3$4 and U_L31 promote the late maturation of viral replication compartments to the nuclear periphery. J. Virol. **78:**5591–5600.
62. **Simpson-Holley, M., R. C. Colgrove, G. Nalepa, J. W. Harper, and D. M. Knipe.** 2005. Identification and functional evaluation of cellular and viral factors involved in the alteration of nuclear architecture during herpes simplex virus 1 infection. J. Virol. **79:**12840–12851.
63. **Wagenaar, F., J. M. Pol, B. Peeters, A. L. Gielkens, N. de Wind, and T. G. Kimman.** 1995. The US3-encoded protein kinase from pseudorabies virus affects egress of virions from the nucleus. J. Gen. Virol. **76:**1851–1859.
64. **Wilkinson, F. L., J. M. Holaska, Z. Zhang, A. Sharma, S. Manilal, I. Holt, S. Stamm, K. L. Wilson, and G. E. Morris.** 2003. Emerin interacts in vitro with the splicing-associated factor, YT521-B. Eur. J. Biochem. **270:**2459–2466.
65. **Worman, H. J., and J. C. Courvalin.** 2005. Nuclear envelope, nuclear lamina, and inherited disease. Int. Rev. Cytol. **246:**231–279.
66. **Yamauchi, Y., C. Shiba, F. Goshima, A. Nawa, T. Murata, and Y. Nishiyama.** 2001. Herpes simplex virus type 2 UL34 protein requires UL31 protein for its relocation to the internal nuclear membrane in transfected cells. J. Gen. Virol. **82:**1423–1428.
67. **Ye, G., K. Vaughan, R. Vallee, and B. Roizman.** 2000. The herpes simplex virus type 1 U_L34 protein interacts with a cytoplasmic dynein intermediate chain and targets nuclear membrane. J. Virol. **74:**1355–1363.